

1993

Direct Measurements of the Transport of Nonequilibrium Electrons in Gold Films with Different Crystal Structures

T. Juhasz


H. E. Elsayed-Ali
Old Dominion University, helsayed@odu.edu

G. O. Smith

C. Suárez

W. E. Bron

Follow this and additional works at: https://digitalcommons.odu.edu/ece_fac_pubs

 Part of the [Condensed Matter Physics Commons](#), and the [Electromagnetics and Photonics Commons](#)

Repository Citation

Juhasz, T.; Elsayed-Ali, H. E.; Smith, G. O.; Suárez, C.; and Bron, W. E., "Direct Measurements of the Transport of Nonequilibrium Electrons in Gold Films with Different Crystal Structures" (1993). *Electrical & Computer Engineering Faculty Publications*. 118.
https://digitalcommons.odu.edu/ece_fac_pubs/118

Original Publication Citation

Juhasz, T., Elsayed-Ali, H. E., Smith, G. O., Suárez, C., & Bron, W. E. (1993). Direct measurements of the transport of nonequilibrium electrons in gold films with different crystal structures. *Physical Review B*, 48(20), 15488-15491. doi:10.1103/PhysRevB.48.15488

Direct measurements of the transport of nonequilibrium electrons in gold films with different crystal structures

T. Juhasz

Department of Physics, University of California, Irvine, California 92717

H. E. Elsayed-Ali

Department of Electrical and Computer Engineering, Old Dominion University, Norfolk, Virginia 23529

G. O. Smith, C. Suárez, and W. E. Bron

Department of Physics, University of California, Irvine, California 92717

(Received 16 July 1993)

The transport of femtosecond-laser-excited nonequilibrium electrons across polycrystalline and single-crystalline gold films has been investigated through time-of-flight measurements. The thicknesses of the films range from 25 to 400 nm. Ballistic electrons as well as electrons interacting with other electrons and/or with the lattice have been observed. The ballistic component dominates the transport in the thinner films, whereas the interactive transport mechanism is dominant at the upper end of the thickness range. A slower effective velocity of the interactive component is observed in the polycrystalline samples, and is assumed to arise from the presence of grain boundaries. The reflection coefficient of excited electrons at the grain boundaries is extracted from the experiment and is estimated to be $r \approx 0.12$. The experiment also suggests that thermal equilibrium among the excited electrons is not fully established in the first ~ 500 fs after excitation.

The dynamics of nonequilibrium electrons in solids has attracted considerable recent attention.¹ Nonequilibrium electrons in metals can be excited by laser pulses with durations less than, or comparable to, the excited-electron energy-loss lifetime (τ_e), such that a transient inequality between the effective electron and lattice temperatures (T_e and T_l) occurs. The excited electron population can be probed through measurements of the transient differential reflectivity (or transmissivity) of the sample. Loss of electron energy in the excited volume is attributed to energy transfer to the lattice through electron-phonon interactions plus electron transport out of the excited region. It has been shown that the relaxation of the nonequilibrium electrons is influenced by the crystal structure of the films, and by the consequent enhanced electron-phonon scattering in the polycrystalline films.² It has been established on experimental and theoretical grounds that electron-grain boundary interactions impede electron transport in polycrystalline films.^{3,4} Earlier experiments on this topic investigated electrons thermalized with the lattice through measurements of the temperature dependence of the resistivity of thin polycrystalline films.⁵ Unresolved, however, is the role of grain boundaries in the transport of nonequilibrium electrons in thin metal films. In the present experiment we investigate the transport of femtosecond-laser-generated nonequilibrium electrons in polycrystalline and single-crystalline gold films, through measurements of the time-of-flight across the film thickness which is made possible through an application of a thermoreflectivity technique with femtosecond resolution.⁶

A synchronously pumped femtosecond dye laser⁷ with output pulses of ~ 150 fs duration at 2-eV photon energy and 76-MHz repetition rate is used to excite the electrons with $\sim 100\text{-}\mu\text{J}/\text{cm}^2$ fluence per pulse on the front surface

of the films. The beam is at near normal incidence and is focused to a diameter of $15 \pm 2 \mu\text{m}$. The skin depth $D \approx 15$ nm. Since an excitation gradient is generated between the skin depth and the rest of the sample, transport of the nonequilibrium electrons out of the excited volume occurs simultaneously with electron energy relaxation through electron-electron and electron-phonon interactions. Excited electrons which reach the back surface of the film introduce a change in the optical reflectivity which is probed with an appropriately delayed laser pulse. The probe beam is also at near normal incidence and is focused to the same diameter as the pump beam, but its intensity is always less than 10% of that of the pump beam. The intensity of the pump beam is modulated with an acousto-optic modulator and the differential reflectivity $[\Delta R/R(t)]$ is detected with a lock-in amplifier tuned to the modulation frequency.

In transient thermoreflectivity experiments the change of reflectivity is related to the change in the occupation number of electrons near the Fermi level.⁸ The occupation number is probed by monitoring the transition probability from the d band to near the Fermi level.⁸ Since the electron occupation number is not a linear function of the effective electron temperature, the change of the reflectivity is generally not proportional to the effective electron temperature at the surface.⁹ The nonlinearity becomes appreciable at lower ambient temperatures and large effective temperature excursions.⁹ Since the present experiment is performed at room temperature with relatively small pump laser irradiance, we assume a linear correspondence between the effective electron temperature and the transient change in $\Delta R/T(t)$. Effects other than changes in the effective electron temperature, such as shifting of the Fermi level, and thermal expansion of the lattice, can also cause reflectivity change, but they are

not significant on the femtosecond time scale.¹⁰ Following standard practices,^{1,2,6,8,9} corrections for the depth-dependent contribution to $\Delta R/R(t)$ (Refs 11 and 12) are ignored in the data analyses.

The gold films are fabricated by evaporation. The film thickness W is determined by a crystal thickness monitor with an estimated absolute accuracy of better than $\pm 20\%$. However the accuracy of the film thicknesses relative to each other is expected to be much better. Polycrystalline gold films are evaporated on ~ 1 -mm-thick sapphire substrates. Examination of films evaporated on an electron microscope grid adjacent to the sapphire substrate reveals a wide distribution of grain sizes with an average of $a_p = 16 \pm 2$ nm. Single-crystalline gold films are fabricated by epitaxial growth on a ~ 2 -nm silver layer grown on a heated NaCl crystal. The film is floated on distilled water, washed in sulfuric acid to remove silver and silver-gold alloy, then washed in distilled water. Finally the film is caught on a sapphire substrate. Electron diffraction obtained from these films shows a single crystal pattern in the (100) orientation. These films are known to possess high dislocation densities (10^{10} – $10^{11}/\text{cm}^3$) and twins.¹³

The transient thermorefectivity [$\Delta R/R(t)$] normalized to its maximum value, and as measured on the back surface of the polycrystalline gold film samples, with thicknesses of 25, 100, 200, 300, and 400 nm, are displayed in Fig. 1. Similar results obtained on single-crystalline films are displayed in Fig. 2. As the thickness of the films is increased the traversal time of the electrons to cross the film, and therefore the delay in the transient $\Delta R/R(t)$, is increased. The short delay times which are observed indicate that energy is transported via electrons, which are out of equilibrium with the lattice.⁶ It is also important to note that the time to reach the maximum value of the transient $\Delta R/R(t)$, relative to its onset, also increases with increasing sample thickness of the polycrystalline samples. This effect is considerably smaller in the single-crystalline samples with thicknesses less than

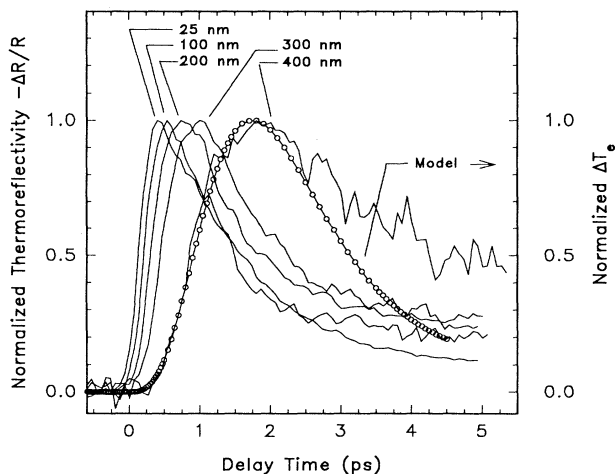


FIG. 1. The normalized transient thermorefectivity signal $\Delta R/R(t)$ measured at the back surface of 25-, 100-, 200-, 300-, and 400-nm-thick polycrystalline gold films. The open circles represent the one-parameter fit of Eqs. (1a) and (1b) to data obtained in the 400-nm-thick films.

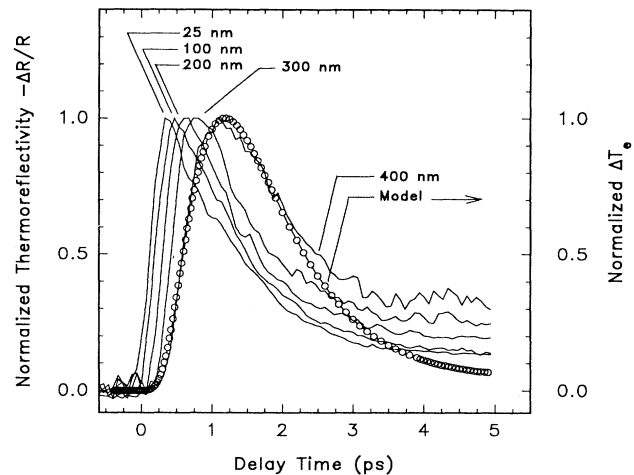


FIG. 2. The normalized transient thermorefectivity signal $\Delta R/R(t)$ measured at the back surface of 25-, 100-, 200-, 300-, and 400-nm-thick single-crystalline gold films. The open circles represent the one-parameter fit of Eqs. (1a) and (1b) to data obtained in the 400-nm-thick films.

400 nm. In order to measure the time required by the first wave of electrons to traverse the films, we measured the time to reach the signal onset of $\Delta R/R(t)$, relative to the excitation at $t=0$, for different sample thicknesses. For simplicity we assign the onset as 15% of the full signal level. The open symbols in Fig. 3 display the results. The circles and triangles represent the polycrystalline and single-crystalline samples, respectively. For each film thickness, the delay of the peak of $\Delta R/R(t)$ corresponds to the time required for the bulk of the excited electrons to reach the back surface. Measurements determining this delay (relative to $t=0$) in both polycrystalline and single-crystalline gold films are displayed by the filled symbols in Fig. 3.

As can be seen in Fig. 3, the time for the first wave of electrons to traverse the films is linear with sample thickness for both polycrystalline and single-crystalline films if the thickness is less than or equal to 300 nm. The linear dependence of the traversal time on the sample thickness is characteristic of ballistic transport, when the transport of the excited electrons occurs without any interactions among the electrons or between the electrons and the lattice. The velocity of the ballistic component is measured to be $\approx 10^6$ m/s in agreement with previously published values.⁶ In the case of the peak of $\Delta R/R(t)$ a linear dependence of the traversal times is observed for shorter thicknesses, namely, up to 100 nm in both types of the gold films. In the 400-nm-thick samples deviations from the linear dependence are observed for the onsets as well as for the peaks in both types of the gold films.

We interpret these results as follows. The transport of the excited electrons across the films with thicknesses less than or equal to 100 nm is mostly ballistic in both single-crystalline and polycrystalline materials. As the thickness of the film increases the fraction of the ballistic component decreases, and the excess energy is carried by electrons interacting with other electrons or/and with the lattice. The electrons undergo one or more scattering events, and we refer to them as the interactive component

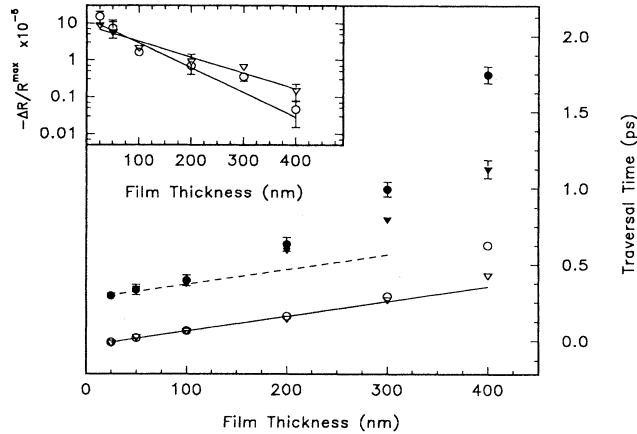


FIG. 3. The delay of the onset of the back surface $\Delta R/R(t)$ as a function of the sample thickness measured at 15% of the full signal intensity (open symbols), and at the peak (filled symbols). The circles and triangles represent the data obtained in polycrystalline and single-crystalline films, respectively. Each data point is an average of four to six measurements, the error bars represent the standard deviations. Solid line, line fit for the first five experimental data points. Dashed line, parallel to the solid line for the benefit of the reader. Inset, the maximum of the back surface thermoreflectivity signal as a function of the sample thickness $\Delta R/R^{\max}(W)$ for polycrystalline and single-crystalline gold films. Solid line, the two-parameter fit of the $a \exp(-W/l)$ function to the data points.

of the transport. Interactive transport also includes the possibility of pure diffusion. Due to the scattering events the interactive electrons lose some of their excess energy during the transport. Since the interactive electrons arrive at the back surface of the sample later than the ballistic electrons, the appearance of the peak of the transient $\Delta R/R(t)$ signal is somewhat delayed. The effect is observed to be stronger in the polycrystalline samples,¹⁴ which indicates that the grain boundaries cause a slowing of the transport of the excited electrons. In samples with 400 nm thicknesses the ballistic component is diminished in both polycrystalline and single-crystalline samples.

We now turn to a quantitative analysis of the experimental results. The dynamics of the excited electrons can be modeled by a set of coupled differential equations, which are frequently referred to as “the two-temperatures model”:¹⁵

$$C_e(T_e) \partial T_e / \partial t = \nabla(\kappa \nabla T_e) - G(T_e - T_l) + P(z, t), \quad (1a)$$

$$C_l \partial T_l / \partial t = G(T_e - T_l), \quad (1b)$$

where $C_e(T_e)$ is the electronic heat capacity (usually assumed to vary linearly with T_e), κ is the electronic thermal conductivity, G is the electron-phonon coupling parameter, $P(z, t)$ is the spatial and temporal evolution of the irradiance of the exciting laser pulse, and C_l is the heat capacity of the lattice. The use of Eqs. (1a) and (1b), however, requires the establishment of an electron temperature T_e . In several experiments which investigated the dynamics of laser excited hot electrons, it was generally assumed that the electron system thermalizes very

rapidly so that an electron temperature exists within the time resolution of the experiments which is ~ 100 fs.¹ On the other hand, it has also been suggested by several authors that the time scales for electron thermalization and for electron-phonon energy transfer may overlap, and therefore, the electron temperature may not be well defined.^{9,12,16} Recently Fann *et al.* have demonstrated that the thermalization of the hot electrons in gold can be as long as ~ 670 fs under special circumstances.^{17,18} An electron thermalization time of ~ 500 fs was measured in the case of weak excitations.¹⁹ The above results impact the interpretation of the present experiment in a number of ways. By definition, the ballistic electrons are not in thermal equilibrium. The presence of ballistic component is observed up to ~ 500 fs which means that thermal equilibrium among the electrons is not fully established during this time interval. On the other hand, as is mentioned above, the thermalization time of femtosecond laser excited nonequilibrium electrons has been independently observed to be about 500 fs.^{17–19} This is supported by our results that ballistic electrons were not observed in samples with thicknesses of 400 nm in which the traversal time of the electrons is ~ 500 fs or longer. In order to move the analysis beyond this point we assume a thermal equilibrium among the electrons arriving at the back surface of the 400-nm-thick films as well as a pure diffusive transport of these electrons. We numerically solve Eqs. (1a) and (1b) for the back surface T_e in the 400-nm-thick samples using the method described in Ref. 20. The electronic heat capacity $C_e(T_e) = 66 \text{ J/m}^3 \text{ K}^2 \times T_e$ for gold,²¹ and the electron-phonon coupling constant is $G = 3.5 \times 10^{16} \text{ W/m}^3 \text{ K}$ for single-crystalline films and $G = 4 \times 10^{16} \text{ W/m}^3 \text{ K}$ for polycrystalline films according to Ref. 2. The diffusion coefficient κ is treated as a parameter. The best agreement with the experimental data is found at $\kappa_s = 310 \text{ W/mK}$ in the case of single-crystalline films, while for polycrystalline films $\kappa_p = 180 \text{ W/mK}$ provided the best solution. The results of the calculations, $\Delta T_e = T_e(t) - T_{\text{ambient}}$, are displayed with open circles in Figs. 1 and 2. Since the calculations are limited to T_e at the back surface of the films, the agreement with the experiment decreases for delays larger than ~ 2 ps beyond which the influence of the effective lattice temperature on $\Delta R/R(t)$ is not negligible.

The difference in the transport of nonequilibrium electrons across single-crystalline and polycrystalline films is also demonstrated by measuring the intensity of the maximum of the transient thermoreflectivity at the back surface as the function of the film thickness. The results, $\Delta R/R^{\max}(W)$, for polycrystalline and single-crystalline samples are displayed in the inset of Fig. 3. An approximately exponential decay of the magnitude of the transient thermoreflectivity is observed in both samples. A somewhat stronger decrease in $\Delta R/R^{\max}(W)$ is observed in the polycrystalline versus the single-crystalline samples,¹⁴ supporting the results obtained by measuring the transversal time of the electrons. This observation is also consistent with previous experiments² in which an enhanced electron cooling rate was observed in polycrystalline films and, hence, the energy transported by the

electrons is expected to decrease.

Finally we discuss our experiment in the terms of the Mayadas-Shatzkes model of the electron transport in polycrystalline metals.³ In this model the grain boundaries are represented by parallel planes separated randomly with an average distance of d . The grain boundaries are assumed to partially reflect the electrons with a reflection coefficient r . It is also assumed that grain boundary scattering occurs simultaneously with an isotropic scattering background (due to electron-electron and electron-phonon interactions), and the interplanar spacing d can be identified as the average grain diameter a_p ($d = a_p$). Under these circumstances Tellier and co-workers^{22,23} have shown that transport in the polycrystalline films can be described by an effective mean free path l_p . We refer to this as the Mayadas-Shatzkes-Tellier (MST) model, and express the effective mean free path as

$$l_p/l_s = f(\alpha) = 1 - \frac{3}{2}\alpha + 3\alpha^2 - 3\alpha^2 \ln(1 + 1/\alpha), \quad (2)$$

where l_s is the bulk mean free path in the single-crystalline material and

$$\alpha = (l_s/a_p)[r/(1-r)]. \quad (3)$$

It follows from Eqs. (2) and (3) that the reflection coefficient of the electrons at the grain boundaries can be determined if l_p and l_s are known. The mean free path of the electrons could be calculated from the electronic thermal conductivity if an electronic temperature exists. Since this is not generally the case, we adopt an empirical approach described in Ref. 24. Specifically we fit $a \exp(-W/l)$ to the back surface $\Delta R/R^{\max}(W)$ signal displayed in the inset of Fig. 3, and define l as an average mean free path of the excited electrons. The method yields $l_p \approx 34$ nm and $l_s \approx 54$ nm for the polycrystalline and single-crystalline films, respectively. Substituting l_p and l_s into Eqs. (2) and (3), we obtain an estimate of $r \approx 0.12$ for the reflection coefficient of nonequilibrium electrons excited in the present experiment. At this point

it would be interesting to compare this value with that obtained with electrons thermalized with the lattice. However, to the best of our knowledge, there are no data available for gold. On the other hand, the grain boundary reflection coefficients in Al ($r=0.17$) and in Cu ($r=0.24$) obtained by electric current measurements^{3,25} appear to be higher.

In summary femtosecond time-of-flight experiments on thin gold films, with different crystal structures, have been carried out in order to investigate the transport of nonequilibrium electrons. The results indicate the presence of both ballistic and interactive components. The ballistic component dominates the transport in thin samples. The dominant role of the ballistic component decreases with increasing sample thickness. For samples thicker than 300 nm the transport is purely interactive. Additionally, the effective velocity of the interactive transport in the polycrystalline samples is observed to be somewhat slower than that in the single-crystalline samples. If one assumes that at the back surface of the thickest samples an electronic temperature and diffusive transport exist, it becomes possible to apply the "two-temperature model" and to determine the coefficient of the electronic thermal conductivity which appears to be larger for single-crystalline films as compared to the polycrystalline films. The difference can be explained by the reflection of the excited electrons at the grain boundaries. Analyzing the results in the terms of the MST model permits an estimate of the reflection coefficient (r) of the electrons at the grain boundaries to be ~ 0.12 . The coefficient is slightly smaller than the values of r in Al and Cu obtained with a different experiment technique.

This research was supported through NSF Grant No. DMR-89-13289, and DOE Grant No. DE-FG0288ER45376. The authors acknowledge Dr. T. Q. Qiu and Professor Y. B. Levinson for helpful discussions.

¹For example, H. E. Elsayed-Ali *et al.*, Phys. Rev. Lett. **58**, 1212 (1987); R. H. M. Groenvelde *et al.*, *ibid.* **64**, 784 (1990); S. D. Brorson *et al.*, *ibid.* **64**, 2172 (1990); M. Van Exter and A. Lagendijk, *ibid.* **60**, 49 (1988); G. L. Eesley *et al.*, *ibid.* **65**, 3445 (1990).

²H. E. Elsayed-Ali *et al.*, Phys. Rev. B **43**, 4488 (1991).

³A. F. Mayadas and M. Shatzkes, Phys. Rev. B **1**, 1382 (1970).

⁴J. Vaneca *et al.*, Thin Solid Films **121**, 201 (1984); G. Reiss *et al.*, Phys. Rev. Lett. **56**, 2100 (1986).

⁵S. K. Bandyopadhyay and A. K. Pal, J. Phys. D **12**, 953 (1979).

⁶S. D. Brorson *et al.*, Phys. Rev. Lett. **59**, 1962 (1987).

⁷T. Juhasz *et al.*, IEEE J. Quantum Electron. **25**, 1704 (1989).

⁸G. L. Eesley, Phys. Rev. **33**, 2144 (1986).

⁹T. Juhasz *et al.*, Phys. Rev. B **45**, 13 819 (1992).

¹⁰R. W. Schoenlein *et al.*, Phys. Rev. Lett. **58**, 1680 (1987).

¹¹A. Miklos and A. Lorincz, J. Appl. Phys. **63**, 2391 (1988); Appl. Phys. B **48**, 261 (1989).

¹²A. Lorincz *et al.*, J. Appl. Phys. **70**, 941 (1991).

¹³G. A. Basset *et al.*, in *Structure and Properties of Thin Films*, edited by C. A. Neugebauer, J. B. Newkirk, and D. A. Vermilyena (Wiley, New York, 1959), p. 11.

¹⁴The absorbed laser power was measured to be within a 5% agreement in the two types of gold films, with slightly more absorption in the polycrystalline films (see Ref. 2). Therefore, variations in the power deposition into the different types of gold films cannot be accounted for in the observed differences.

¹⁵S. I. Anisimov *et al.*, Zh. Eksp. Teor. Fiz. **66**, 776 (1974) [Sov. Phys. JETP **39**, 375 (1974)].

¹⁶M. B. Agranat *et al.*, Appl. Phys. B **47**, 209 (1988).

¹⁷W. S. Fann *et al.*, Phys. Rev. Lett. **68**, 2834 (1992).

¹⁸W. S. Fann *et al.*, Phys. Rev. B **46**, 13 592 (1992).

¹⁹F. Vallee, C. K. Sun, L. Acioli, E. P. Ippen, and J. G. Fujimoto OSA Tech. Dig. Ser. **12**, 69 (1993).

²⁰T. Q. Qui and C. L. Tien, Int. J. Heat Mass Transfer **35**, 719 (1992).

²¹*American Institute of Physics Handbook*, 3rd ed., edited by D. E. Gray (McGraw-Hill, New York, 1972).

²²C. R. Tellier *et al.*, Thin Solid Films **44**, 201 (1977).

²³C. R. Tellier, Thin Solid Films **51**, 311 (1978).

²⁴S. M. Sze *et al.*, Solid State Electron. **7**, 509 (1964).

²⁵P. V. Andrews, Phys. Lett. **19**, 558 (1965).